

DESIGN OF IMAGE-MATCHED NON-SEPARABLE WAVELET USING CONVOLUTIONAL NEURAL NETWORK

Naushad Ansari*, Anubha Gupta, and Rahul Duggal

SBILab, Deptt. of ECE, IIT-Delhi, India

ABSTRACT

Image-matched nonseparable wavelets can find potential use in many applications including image classification, segmentation, compressive sensing, etc. This paper proposes a novel design methodology that utilizes convolutional neural network (CNN) to design two-channel non-separable wavelet matched to a given image. The design is proposed on quincunx lattice. The loss function of the convolutional neural network is setup with total squared error between the given input image to CNN and the reconstructed image at the output of CNN, leading to perfect reconstruction at the end of training. Simulation results have been shown on some standard images.

Index Terms— Nonseparable wavelet, Quincunx lattice, Convolutional Neural Network

1. INTRODUCTION

Over the past three decades, wavelets have been found utility in a number of applications spanning different disciplines including geoscience engineering, image processing applications, signal processing, etc. [1–9]. In particular, choosing an appropriate wavelet in image segmentation, classification, compressive sensing, and similar applications, is generally a great challenge. There exist more number of standard wavelets for one-dimensional signals than the nonseparable wavelets for images because the latter are difficult to design. Hence, often one-dimensional wavelets are used as separable wavelets in image processing applications. However, there may be inter-dependence of information along different directions. Hence, a non-separable image-matched wavelet may provide better results in applications compared to a standard separable wavelet.

Although a number of methods have been proposed for the design of multidimensional wavelets [8, 10–17], these have, largely, been designed irrespective of signal of interest. In [18], statistically matched non-separable wavelets have been designed for a class of images belonging to fractional Brownian field. The method first designs highpass filter using the signal statistics followed by the conditions of perfect

reconstruction to design three other filters required for a 2-channel nonseparable wavelet system. Thus, [18] designs only one filter matched to the class of images. Also, the designed wavelets are matched to images, while this paper focuses on designing a wavelet that is matched to a given image.

This paper proposes a novel methodology that designs two-channel nonseparable wavelet from a given image using the convolutional neural network (CNN). The design methodology is simple and easy to use for the design of image-matched nonseparable wavelet. Since a two-channel wavelet is designed, CNN has an architecture similar to a 2 channel filterbank. The squared error between the input image and the CNN output image is used as the loss function and is propagated back until the loss function falls considerably low or the PSNR of the reconstructed image increases beyond 70dB.

This paper is organized in four sections. Section 2 briefly reviews the basic concepts of nonseparable wavelets. Section 3 presents the proposed convolutional neural network based approach for the design of image-matched two channel non-separable wavelet. This section also presents simulation results on some images. In the end, conclusions are presented in section 4.

Notations: We use lowercase bold letters and uppercase bold letters to represent 2-dimensional (2-D) vectors and 2×2 matrices, respectively. Thus, a discrete 2-D signal is denoted by $a[n]$ where $n = (n_1, n_2)$. The scalar variables are represented by lowercase italicized letters.

2. BRIEF BACKGROUND ON NONSEPARABLE WAVELETS

Consider a 2-band nonseparable wavelet system shown in Figure-1. A two channel nonseparable wavelet system consists of four 2-dimensional filters, labeled as, \mathbf{h}_0 , \mathbf{h}_1 , \mathbf{f}_0 , and \mathbf{f}_1 , where \mathbf{h}_0 and \mathbf{h}_1 are analysis lowpass and highpass filters and, \mathbf{f}_0 and \mathbf{f}_1 are synthesis lowpass and highpass filters, respectively. In the multiresolution approximation corresponding to wavelet system, the scaling subspace is spanned by 2-D integer translates of the associated 2-D scaling function, $\Phi(\mathbf{x})$, defined at that subspace [19]. Similar to the 1-D case, the 2-D scaling function satisfies the recursive, two-scale re-

*Thanks to CSIR, Govt. of India for funding.

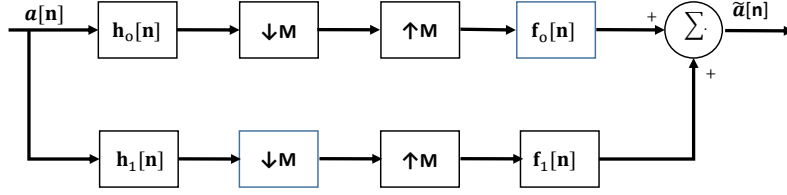


Figure-1: 2-Channel nonseparable wavelet system

relationship of (1). If it exists, then the wavelet function, $\Psi(\mathbf{x})$, satisfies (2).

$$\Phi(\mathbf{x}) = \sum_{\mathbf{n}} \sqrt{|\det(\mathbf{M})|} f_0(\mathbf{n}) \Phi(\mathbf{M}\mathbf{x}-\mathbf{n}) \quad (1)$$

$$\Psi(\mathbf{x}) = \sum_{\mathbf{n}} \sqrt{|\det(\mathbf{M})|} f_1(\mathbf{n}) \Psi(\mathbf{M}\mathbf{x}-\mathbf{n}) \quad (2)$$

where \mathbf{M} is the decimation matrix characterizing the sampling process. Likewise, the dual scaling function $\tilde{\Phi}(\mathbf{x})$ and the dual wavelet function $\tilde{\Psi}(\mathbf{x})$ are related to the analysis filters $\mathbf{h}_0(\mathbf{n})$ and $\mathbf{h}_1(\mathbf{n})$ via similar equations. If $|\det(\mathbf{M})| = 2$, then we obtain a 2-channel nonseparable wavelet system. The theory of nonseparable wavelets requires the use of lattices, where a lattice is the set of all vectors generated by $\mathbf{M}\mathbf{n}$, $\mathbf{n} \in \mathbb{Z}^2$. For the 2-channel case, only quincunx lattice generates MRA and the corresponding decimation matrix generates a rotated rectangular grid. For example, matrix $\mathbf{M} = \begin{bmatrix} 1 & 1 \\ 1 & -1 \end{bmatrix}$ corresponds to the decimation matrix for the quincunx lattice.

3. PROPOSED WORK ON NONSEPARABLE WAVELET DESIGN USING CNN ARCHITECTURE

In this section, we present the proposed design on image-matched nonseparable wavelet. We use the convolutional neural network architecture for quincunx wavelet design.

3.1. Proposed Design

Consider Figure-2 that shows the CNN architecture based proposed wavelet design. The CNN network has two layers of two filters each. Each layer is trained with the gradient of loss function received from the output via back propagation. The loss function is setup as the squared error between the input applied image and the output reconstructed image as shown in Figure-2. After layer-1 output, an operation similar to pooling is applied wherein alternate image samples are replaced with zeros (Figure-2), implementing downsampling and upsampling by \mathbf{M} of the corresponding wavelet structure. Layer-1 filters correspond to analysis filters and layer-2 filters correspond to synthesis filter.

The steps for the design are as below:

1. The given image is applied as the input to the CNN architecture.
2. All the filters are initialized as shown in Table-1. A 2-channel wavelet system is implemented with lowpass and highpass filters. Hence, instead of a random initialization, filters have been initialized to small-sized lowpass and highpass filters.
3. Loss function at the output is computed as

$$L = \sum_{\mathbf{n}} (\mathbf{a}[\mathbf{n}] - \tilde{\mathbf{a}}[\mathbf{n}])^2 \quad (3)$$

where $\mathbf{a}[\mathbf{n}]$ denotes the input image, $\tilde{\mathbf{a}}[\mathbf{n}]$ denotes the reconstructed image, and the summation is done for the entire size of the input image. In this work, we have considered two 512×512 sized raw BMP images.

4. Once initialized, the CNN training is started wherein the gradient of loss function is propagated back to all the four filters and the network is trained using back-propagation (BP) algorithms leading to perfect reconstruction at the output at the end of training.

3.2. Simulation Results

Results are presented over two images: Lena and Barbara shown in Figure-3.



Figure-3: Images Used

Table-1: Filter Initialization

	Lena						Barbara				
$h_0 =$	0.001283	0.007166	-0.00292	0.006442	0.000872	$h_0 =$	0.002001	0.010625	-0.00088	0.011605	0.002317
	0.001994	-0.01476	-0.01511	-0.01313	0.004139		-0.00047	-0.02004	-0.02562	-0.01926	-0.00607
	0.003217	-0.04395	0.16053	-0.04389	0.00087		0.006187	-0.02934	0.17	-0.03002	0.010321
	-0.02683	0.14847	0.67797	0.14944	-0.02605		-0.04546	0.1309	0.67046	0.13229	-0.04439
	-0.00146	-0.04581	0.157	-0.04543	-0.00083		0.004737	-0.03008	0.16248	-0.03214	0.003057
	0.004766	-0.01761	-0.01907	-0.01831	0.004197		-0.00367	-0.02006	-0.02639	-0.02474	-0.00197
$h_1 =$	0.009191	0.024461	-0.0119	0.021247	0.006269	$h_1 =$	0.004402	0.016384	-0.00881	0.01658	0.010508
	0.01668	-0.03177	-0.29928	-0.03298	0.014218		0.02539	-0.00954	-0.27629	-0.00778	0.021937
	-0.01444	-0.29162	1.1916	-0.29154	-0.01522		-0.00786	-0.29906	1.1827	-0.30011	-0.01056
	0.011849	-0.03651	-0.30265	-0.03655	0.01165		0.019448	-0.01273	-0.28138	-0.00942	0.022713
	0.002763	0.01124	-0.02476	0.01418	0.00228		-0.00033	0.006827	-0.03747	0.006146	0.00288
	0.00024	0.007348	0.004781	0.005939	0.000716		0.002141	0.01197	0.001217	0.013167	-0.00381
$f_0 =$	0.009134	-0.03105	-0.02055	-0.02902	0.005302	$f_0 =$	0.005269	-0.0377	-0.02098	-0.04019	0.008903
	-0.01915	-0.04309	0.29385	-0.04438	-0.01733		-0.00833	-0.03082	0.3053	-0.03098	-0.00481
	-0.01381	0.28628	1.1935	0.28598	-0.01518		0.009126	0.25363	1.1912	0.25502	0.006129
	-0.0133	-0.04325	0.30231	-0.04393	-0.01369		0.000547	-0.03778	0.31715	-0.03346	-0.00511
	0.003028	-0.01243	-0.01996	-0.01329	0.003902		0.009613	-0.02307	-0.01547	-0.02154	0.010683
	0.000761	0.00921	-0.00089	0.009541	0.001294		0.003287	0.011787	0.007703	0.012524	0.006862
$f_1 =$	-0.00176	0.007302	0.004923	0.007224	-0.00139	$f_1 =$	-0.00011	0.010445	0.011473	0.010973	0.001746
	0.001632	0.018108	-0.02151	0.016197	0.003127		-0.00172	0.014811	-0.03629	0.013447	-0.00718
	-0.00199	-0.05014	-0.15516	-0.04965	0.000462		0.002001	-0.03917	-0.13814	-0.04121	0.000377
	-0.0272	-0.14558	0.67754	-0.14638	-0.02649		-0.04297	-0.14213	0.66152	-0.14339	-0.04173
	0.001787	-0.0497	-0.15456	-0.05048	0.001254		0.002059	-0.04105	-0.14021	-0.04228	0.002298
	0.003635	0.017711	-0.018	0.018744	0.003887		-0.00557	0.012796	-0.02527	0.017747	-0.00364

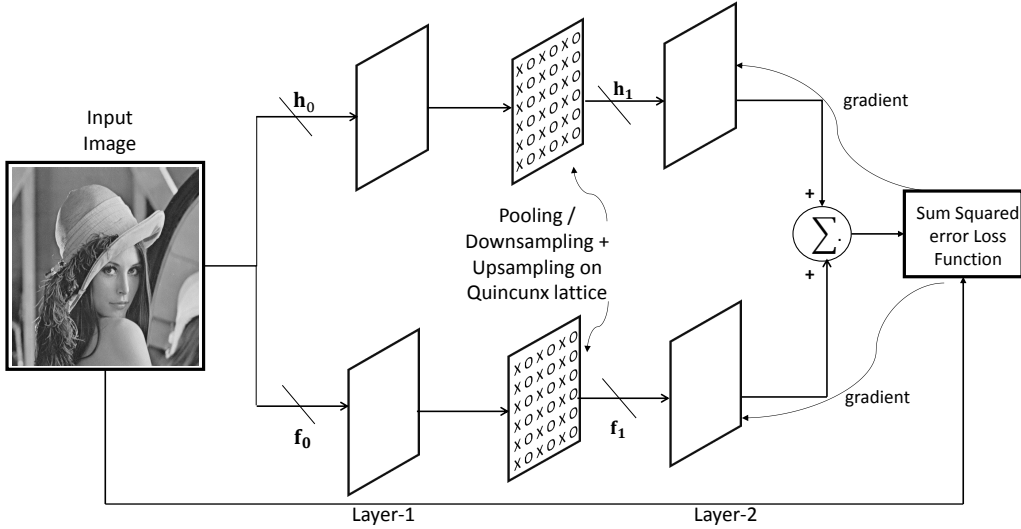


Figure 2: Proposed CNN Architecture for Nonseparable Wavelet Design over Quincunx Lattice
 'x': denotes sample kept, 'o' denotes sample discarded

The CNN network is trained using the learning rate= 2×10^{-7} , using Stochastic Gradient Descent (SGD) with Nesterov momentum with momentum value equal to 0.9. The network got trained for each image in approx. 15000 iterations. Perfect reconstruction is obtained at the end of training, i.e., when the loss function dropped to a very low insignificant value. The designed filters are tabulated in Table-2 and

the corresponding filters are shown in Figure-3.

4. CONCLUSION

This paper proposes a novel methodology for designing a two-channel nonseparable wavelet over quincunx lattice from a given image. Since this wavelet is designed from the given

Table-2: Coefficients of image-matched filters designed using the proposed methodology

	Lena						Barbara				
$\mathbf{h}_0 =$	0.001283	0.007166	-0.00292	0.006442	0.000872	$\mathbf{h}_0 =$	0.002001	0.010625	-0.00088	0.011605	0.002317
	0.001994	-0.01476	-0.01511	-0.01313	0.004139		-0.00047	-0.02004	-0.02562	-0.01926	-0.00607
	0.003217	-0.04395	0.16053	-0.04389	0.00087		0.006187	-0.02934	0.17	-0.03002	0.010321
	-0.02683	0.14847	0.67797	0.14944	-0.02605		-0.04546	0.1309	0.67046	0.13229	-0.04439
	-0.00146	-0.04581	0.157	-0.04543	-0.00083		0.004737	-0.03008	0.16248	-0.03214	0.003057
	0.004766	-0.01761	-0.01907	-0.01831	0.004197		-0.00367	-0.02006	-0.02639	-0.02474	-0.00197
$\mathbf{h}_1 =$	0.009191	0.024461	-0.0119	0.021247	0.006269	$\mathbf{h}_1 =$	0.004402	0.016384	-0.00881	0.01658	0.010508
	0.01668	-0.03177	-0.29928	-0.03298	0.014218		0.02539	-0.00954	-0.27629	-0.00778	0.021937
	-0.01444	-0.29162	1.1916	-0.29154	-0.01522		-0.00786	-0.29906	1.1827	-0.30011	-0.01056
	0.011849	-0.03651	-0.30265	-0.03655	0.01165		0.019448	-0.01273	-0.28138	-0.00942	0.022713
	0.002763	0.01124	-0.02476	0.01418	0.00228		-0.00033	0.006827	-0.03747	0.006146	0.00288
	0.00024	0.007348	0.004781	0.005939	0.000716		0.002141	0.01197	0.001217	0.013167	-0.00381
$\mathbf{f}_0 =$	0.009134	-0.03105	-0.02055	-0.02902	0.005302	$\mathbf{f}_0 =$	0.005269	-0.0377	-0.02098	-0.04019	0.008903
	-0.01915	-0.04309	0.29385	-0.04438	-0.01733		-0.00833	-0.03082	0.3053	-0.03098	-0.00481
	-0.01381	0.28628	1.1935	0.28598	-0.01518		0.009126	0.25363	1.1912	0.25502	0.006129
	-0.0133	-0.04325	0.30231	-0.04393	-0.01369		0.000547	-0.03778	0.31715	-0.03346	-0.00511
	0.003028	-0.01243	-0.01996	-0.01329	0.003902		0.009613	-0.02307	-0.01547	-0.02154	0.010683
	0.000761	0.00921	-0.00089	0.009541	0.001294		0.003287	0.011787	0.007703	0.012524	0.006862
$\mathbf{f}_1 =$	-0.00176	0.007302	0.004923	0.007224	-0.00139	$\mathbf{f}_1 =$	-0.00011	0.010445	0.011473	0.010973	0.001746
	0.001632	0.018108	-0.02151	0.016197	0.003127		-0.00172	0.014811	-0.03629	0.013447	-0.00718
	-0.00199	-0.05014	-0.15516	-0.04965	0.000462		0.002001	-0.03917	-0.13814	-0.04121	0.000377
	-0.0272	-0.14558	0.67754	-0.14638	-0.02649		-0.04297	-0.14213	0.66152	-0.14339	-0.04173
	0.001787	-0.0497	-0.15456	-0.05048	0.001254		0.002059	-0.04105	-0.14021	-0.04228	0.002298
	0.003635	0.017711	-0.018	0.018744	0.003887		-0.00557	0.012796	-0.02527	0.017747	-0.00364

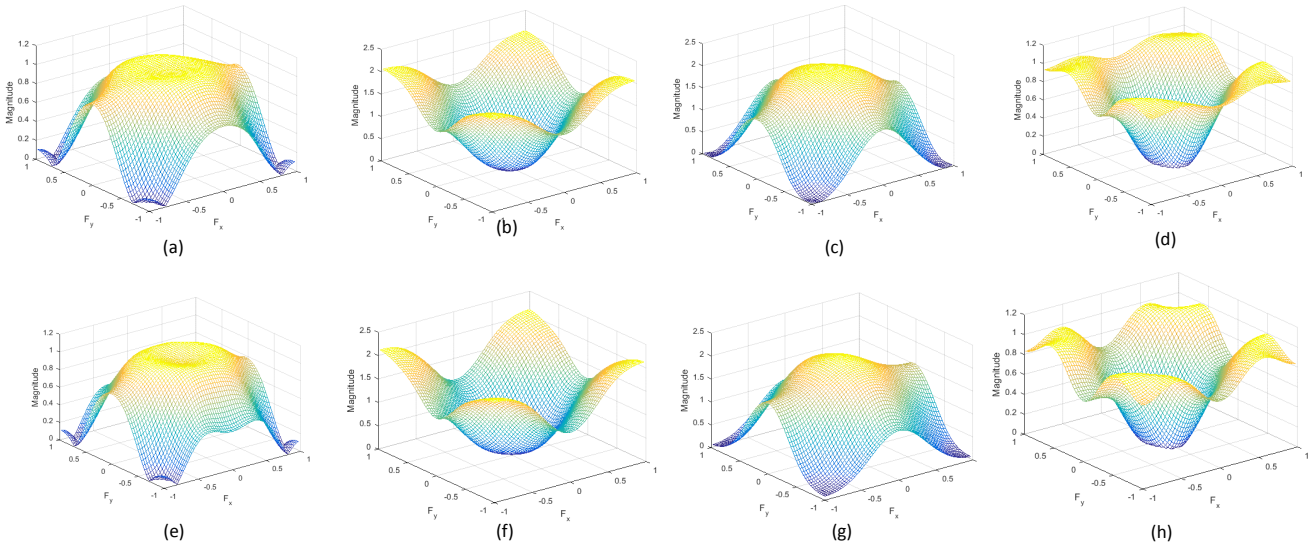


Figure-4: Image-matched filters designed using the proposed methodology; Lena image: (a) \mathbf{h}_0 , (b) \mathbf{h}_1 , (c) \mathbf{f}_0 , and (d) \mathbf{f}_1 ; Barbara Image: (e) \mathbf{h}_0 , (f) \mathbf{h}_1 , (g) \mathbf{f}_0 , and (h) \mathbf{f}_1

image itself, it may be able to capture image characteristics/features better than the existing wavelets. Hence, this design methodology can find potential use in image processing applications. In the future, this design will be extended to 3-dimensional wavelet design and will be explored in applications of classification and segmentation.

5. REFERENCES

- [1] P. Abry, S. G. Roux, H. Wendt, P. Messier, A. G. Klein, N. Tremblay, P. Borgnat, S. Jaffard, B. Vedel, J. Codding *et al.*, "Multiscale anisotropic texture analysis and classification of photographic prints: Art scholar-

- ship meets image processing algorithms,” *IEEE Signal Processing Magazine*, vol. 32, no. 4, pp. 18–27, 2015.
- [2] B. Pradhan, M. N. Jebur, H. Z. M. Shafri, and M. S. Tehrani, “Data fusion technique using wavelet transform and taguchi methods for automatic landslide detection from airborne laser scanning data and quickbird satellite imagery,” *IEEE Transactions on Geoscience and Remote Sensing*, vol. 54, no. 3, pp. 1610–1622, 2016.
- [3] Y. Y. Tang, Y. Lu, and H. Yuan, “Hyperspectral image classification based on three-dimensional scattering wavelet transform,” *IEEE Transactions on Geoscience and Remote Sensing*, vol. 53, no. 5, pp. 2467–2480, 2015.
- [4] M. Sakkari and M. Zaied, “An architecture of distributed beta wavelet networks for large image classification in mapreduce,” in *2015 15th International Conference on Intelligent Systems Design and Applications (ISDA)*. IEEE, 2015, pp. 523–527.
- [5] P. Cirujeda, H. Müller, D. Rubin, T. A. Aguilera, B. W. Loo, M. Diehn, X. Binefa, and A. Depeursinge, “3d riesz-wavelet based covariance descriptors for texture classification of lung nodule tissue in ct,” in *2015 37th Annual International Conference of the IEEE Engineering in Medicine and Biology Society (EMBC)*. IEEE, 2015, pp. 7909–7912.
- [6] K. Jiang, Z. Zhou, X. Geng, X. Zhang, L. Tang, H. Wu, and J. Dong, “Isotropic undecimated wavelet transform fuzzy algorithm for retinal blood vessel segmentation,” *Journal of Medical Imaging and Health Informatics*, vol. 5, no. 7, pp. 1524–1527, 2015.
- [7] M. Unser, “Wavelets: on the virtues and applications of the mathematical microscope,” *Journal of microscopy*, vol. 255, no. 3, pp. 123–127, 2014.
- [8] Z. Püspöki, V. Uhlmann, C. Vonesch, and M. Unser, “Design of steerable wavelets to detect multifold junctions,” *IEEE Transactions on Image Processing*, vol. 25, no. 2, pp. 643–657, 2016.
- [9] S. Kumar, R. Gupta, N. Khanna, S. Chaudhury, and S. D. Joshi, “Text extraction and document image segmentation using matched wavelets and mrf model,” *IEEE Transactions on Image Processing*, vol. 16, no. 8, pp. 2117–2128, 2007.
- [10] J. Zhou, M. N. Do, and J. Kovacevic, “Multidimensional orthogonal filter bank characterization and design using the cayley transform,” *IEEE Transactions on image processing*, vol. 14, no. 6, pp. 760–769, 2005.
- [11] Y. M. Lu and M. N. Do, “Multidimensional directional filter banks and surfacelets,” *IEEE Transactions on Image Processing*, vol. 16, no. 4, pp. 918–931, 2007.
- [12] A. M. Ruedin, “Construction of nonseparable multi-wavelets for nonlinear image compression,” *EURASIP Journal on Advances in Signal Processing*, vol. 2002, no. 1, pp. 1–7, 2002.
- [13] D. Wei and S. Guo, “A new approach to the design of multidimensional nonseparable two-channel orthonormal filterbanks and wavelets,” *IEEE Signal Processing Letters*, vol. 7, no. 11, pp. 327–330, 2000.
- [14] J. P. Ward, P. Pad, and M. Unser, “Optimal isotropic wavelets for localized tight frame representations,” *IEEE Signal Processing Letters*, vol. 22, no. 11, pp. 1918–1921, 2015.
- [15] J. Kovacevic and M. Vetterli, “Nonseparable two-and three-dimensional wavelets,” *IEEE Transactions on Signal Processing*, vol. 43, no. 5, pp. 1269–1273, 1995.
- [16] —, “Nonseparable multidimensional perfect reconstruction filter banks and wavelet bases for \mathbb{R}^n ,” *IEEE Transactions on Information Theory*, vol. 38, no. LCAV-ARTICLE-1992-002, pp. 533–555, 1992.
- [17] D. B. Tay and N. G. Kingsbury, “Flexible design of multidimensional perfect reconstruction fir 2-band filters using transformations of variables,” *IEEE Transactions on Image Processing*, vol. 2, no. 4, pp. 466–480, 1993.
- [18] A. Gupta and S. Joshi, “Two-channel nonseparable wavelets statistically matched to 2-d images,” *Signal Processing*, vol. 91, no. 4, pp. 673–689, 2011.
- [19] R. M. Rao and A. S. Bopardikar, “Wavelet transforms: introduction to theory and applications,” 1998.